Bufalin Reverses Resistance to Sorafenib by Inhibiting Akt Activation in Hepatocellular Carcinoma: The Role of Endoplasmic Reticulum Stress

Bo Zhai[1], Fengli Hu[2], Haijiang Yan[1], Dali Zhao[3], Xin Jin[1], Taishi Fang[1], Shangha Pan[3], Xueying Sun[3], Lishan Xu[1]*

1 Department of General Surgery, the Fourth Affiliated Hospital of Harbin Medical University, Harbin, Heilongjiang, China, 2 Department of Gastroenterology, the Fourth Affiliated Hospital of Harbin Medical University, Harbin, Heilongjiang, China, 3 Department of General Surgery, the First Affiliated Hospital of Harbin Medical University, Harbin, Heilongjiang, China

* xulishan001@126.com

Abstract

Sorafenib is the standard first-line therapeutic treatment for patients with advanced hepatocellular carcinoma (HCC), but its use is hampered by the development of drug resistance. The activation of Akt by sorafenib is thought to be responsible for this resistance. Bufalin is the major active ingredient of the traditional Chinese medicine *Chan su*, which inhibits Akt activation; therefore, *Chan su* is currently used in the clinic to treat cancer. The present study aimed to investigate the ability of bufalin to reverse both inherent and acquired resistance to sorafenib. Bufalin synergized with sorafenib to inhibit tumor cell proliferation and induce apoptosis. This effect was at least partially due to the ability of bufalin to inhibit Akt activation by sorafenib. Moreover, the ability of bufalin to inactivate Akt depended on endoplasmic reticulum (ER) stress mediated by inositol-requiring enzyme 1 (IRE1). Silencing IRE1 with siRNA blocked the bufalin-induced Akt inactivation, but silencing eukaryotic initiation factor 2 (eIF2) or C/EBP-homologous protein (CHOP) did not have the same effect. Additionally, silencing Akt did not influence IRE1, CHOP or phosphorylated eIF2α expression. Two sorafenib-resistant HCC cell lines, which were established from human HCC HepG2 and Huh7 cells, were refractory to sorafenib-induced growth inhibition but were sensitive to bufalin. Thus, Bufalin reversed acquired resistance to sorafenib by downregulating phosphorylated Akt in an ER-stress-dependent manner via the IRE1 pathway. These findings warrant further studies to examine the utility of bufalin alone or in combination with sorafenib as a first- or second-line treatment after sorafenib failure for advanced HCC.

Abbreviations: HCC, hepatocellular carcinoma; MAPK, mitogen-activated protein kinase; ERK, extracellular signal-regulated kinase; PI3K, phosphatidylinositol 3-kinase; ER, endoplasmic reticulum; UPR, unfolded protein response; IRE1, inositol-requiring enzyme 1; ATF6, transcription actor 6; eIF2, eukaryotic initiation factor 2; CHOP, C/EBP-homologous protein; DMEM, Dulbecco's modified Eagle's medium; Abs, antibodies; FITC, fluorescein isothiocyanate; DMSO, dimethyl sulfoxide; CCK-8, Cell Counting Kit-8; IC50, half-maximal inhibitory concentration; PI, propidium iodide; PVDF, polyvinylidene difluoride; ANOVA, one-way analysis of variance; CDI, coefficient of drug interaction.

Introduction

Hepatocellular carcinoma (HCC) is the sixth most common cancer worldwide, with more than 700,000 new cases and 700,000 deaths annually [1]. Most HCC patients are diagnosed at the advanced stages; therefore, the need for new systemic therapies is urgent. However, HCC is notoriously resistant to systemic chemotherapy [2]. Sorafenib, a multikinase inhibitor, is the first and only drug that has been approved as the standard first-line systemic treatment for advanced HCC. However, drug resistance to sorafenib is a worrisome phenomenon that is associated with limited survival benefits and very low response rates [3, 4]. Identifying the molecular mechanisms of sorafenib resistance and improving the response of patients to sorafenib are thus important for the treatment of HCC.

Sorafenib not only blocks the Raf/mitogen-activated protein kinase (MAPK)/extracellular signal-regulated kinase (ERK) signaling pathway but also inhibits a number of tyrosine kinase receptors, including the vascular endothelial growth factor and platelet-derived growth factor receptors [3]. However, sorafenib does not directly target the phosphoinositide 3-kinase (PI3K)/Akt pathway, which is critical for the development and progression of HCC and which is activated in 92.3% of HCC specimens [5, 6]. Sorafenib-induced Akt activation has been reported in both sorafenib-resistant and parental HCC cells [7–9]. Although the mechanisms that underlie the role of Akt activation remain unclear, blocking the PI3K/Akt pathway augments the effects of sorafenib and reverses acquired resistance to sorafenib [7, 9, 10].

Anticancer agents should ultimately induce cell death. Tumor cells that are not killed by chemotherapy are considered drug resistant. Generally, primary resistance is initially due to genetic heterogeneity [4]. However, patients who initially respond to therapy often acquire resistance after long-term exposure to antitumor drugs and will eventually progress [11]. Many mechanisms, such as addiction switching, compensatory pathways due to pathway loops or cross-talk, the epithelial-mesenchymal transition, cancer stem cells, the disabling of pro-apoptotic signals, and a hypoxic microenvironment, are involved in apoptotic pathway imbalance, which leads to cell survival and drug resistance [4, 12, 13]. Moreover, endoplasmic reticulum (ER) stress disturbs the normal functions of the ER via the unfolded protein response (UPR), which has caused widespread concern [14–20]. A number of cellular stress conditions, such as nutrient deprivation, hypoxia, and alterations in glycosylation status, lead to the accumulation of unfolded and/or misfolded proteins in the ER lumen and cause so-called ER stress. The initial physiological aim is to restore ER function by reducing the amount of immature proteins, but this approach can eventually trigger ER-stress-mediated apoptosis if ER dysfunction is severe or prolonged. This approach can also trigger cross-talk with many signaling pathways, including PI3K/Akt [15, 21]. The ER stress pathways consist of three main signaling cascades that are facilitated by the following: inositol-requiring kinase 1 (IRE1), activating transcription factor 6 (ATF6) and protein kinase RNA-like ER kinase [22]. Once activated, protein kinase RNA-like ER kinase phosphorylates eukaryotic initiation factor 2 (eIF2) to inhibit protein translation and upregulate ATF4 and C/EBP-homologous protein (CHOP) expression. ATF6 then translocates into the nucleus and induces the expression of genes that contain an ER stress response element, including CHOP [22, 23]. Accumulating evidence indicates that ER stress is activated in various solid tumors and is involved in drug resistance in many different tumor types, including HCC [14–20]. Moreover, acquired drug resistance is induced by antitumor drugs due to the absence of ER stress [20]. Recently, sorafenib was also reported to induce ER-stress-dependent apoptosis in HCC cells [22, 24].

Bufalin, an ingredient of the traditional Chinese medicine *Chan su*, which is obtained from the skin and parotid venom glands of the toad *Bufo bufo gargarizans Cantor*, has been approved by the Chinese State Food and Drug Administration and is widely used to treat

patients with liver, lung, colon and pancreatic cancers at oncology clinics in China [25]. We previously found that bufalin inhibited HCC cell proliferation and induced apoptosis by activating the ER stress response via the IRE1 pathway. We also showed that the molecular mechanism of acquired resistance to sorafenib was Akt activation [7], as inhibition of Akt could enhance antitumor effects [10] and reverse acquired resistance to sorafenib [7]. Importantly, bufalin also suppresses cancer by inhibiting the activation of Akt [26–28]. However, the role of bufalin-induced ER stress and its cross-talk with the PI3K/Akt pathway in mediating HCC resistance to sorafenib has not yet been reported. Herein, we demonstrate that bufalin and sorafenib synergistically act to induce HCC cell death by downregulating phosphorylated (p)-Akt in an ER-stress-dependent manner mediated by the IRE1 pathway. Bufalin also reverses acquired resistance to sorafenib via this mechanism. Therefore, bufalin may help to improve sorafenib treatment by alleviating both inherent and acquired resistance.

Materials and Methods

Cell lines and antibodies

Human HCC HepG2 cells were purchased from the American Type Culture Collection (ATCC; Manassas, VA, USA), and Huh7 cells were obtained from the Chinese Academy of Sciences Cell Bank (Shanghai, China). The cells were routinely cultured at 37°C in Dulbecco's modified Eagle's medium (DMEM) supplemented with 10% fetal bovine serum. Antibodies (Abs) against Akt, p-Akt (Ser473), CHOP, and p-eIF2α were purchased from Cell Signaling Technology (Danvers, MA, USA), and Abs against IRE1 and β-actin were from Santa Cruz Biotechnology (Santa Cruz, CA, USA). In addition, fluorescein isothiocyanate (FITC)-conjugated anti-rabbit secondary Ab and Alexa Fluor 594-conjugated anti-rabbit and anti-mouse secondary Abs were from Zhongshan Golden Bridge Biotechnology (Beijing, China).

Reagents

Bufalin and LY294002 were purchased from Sigma (St. Louis, MO, USA). Sorafenib and perifosine were purchased from Jinan Trio Pharmatech Co., Ltd. (Jinan, China). The bufalin, sorafenib and LY294002 were dissolved in 100% dimethyl sulfoxide (DMSO; Sigma, St. Louis, MO, USA) to prepare stock solutions of 1 mM, 100 mM, and 100 mM, respectively, which were diluted in DMEM to the desired concentrations for the *in vitro* assays. All stock solutions contained a final DMSO concentration of less than 0.1%. Perifosine was dissolved in phosphate-buffered saline to prepare a 30 μM stock solution.

Cell viability assay

Cell viability was analyzed using a Cell Counting Kit-8 (CCK-8) kit (Dojindo Laboratories, Kumamoto, Japan) as described previously [23, 29]. Briefly, the cells were plated in 96-well culture plates at a density of 3×10^3 cells/well and were cultured overnight. The cells were then incubated in fresh culture medium containing bufalin and/or sorafenib at various concentrations for 24 to 72 h. The cell viability was then assessed according to the manufacturer's guidelines. The experiments were repeated in triplicate.

Establishment of sorafenib-resistant cells

The sorafenib-resistant cell lines Huh7-Sora and HepG2-Sora were established by incubating Huh7 and HepG2 cells, respectively, with increasing concentrations of sorafenib, as described previously [7, 30, 31]. The half-maximal inhibitory concentration (IC50) of HCC cells to sorafenib was initially determined, and the cells were then cultured in medium containing sorafenib

at concentrations just below their respective IC50 values. The concentration of sorafenib was slowly increased by 0.25 μmol/L per week. After 6 to 7 months, the cells that were able to survive in the medium containing 10 μM sorafenib were considered to be sorafenib resistant.

Detection of cell apoptosis *in vitro*

Cells were seeded at 5.0×10^5 cells/well in six-well plates, cultured for 48 h, and then harvested. Apoptosis was detected using an Annexin V-FITC/propidium iodide (PI) apoptosis detection kit (BD Biosciences, Beijing, China). Briefly, the cells were incubated with 5 μl of Annexin V and 5 μl of PI for 15 min. The apoptotic cells were then analyzed by flow cytometry (Beckman Coulter, Brea, CA, USA) or viewed under a laser-scanning confocal microscope (LSM-510 Meta, Carl Zeiss Jena) as described previously [23, 32]. The experiments were repeated in triplicate.

Caspase activity assay

The activities of caspase-3 and caspase-9 were measured with caspase-3 and caspase-9 activity kits (Beyotime Institute of Biotechnology, Haimen, Jiangsu, China), respectively, according to the manufacturer's instructions. For this purpose, cells were harvested and lysed, total protein was extracted, and the protein concentration was determined. A mixture of 10 μl of protein extracts, 80 μl of reaction buffer and 10 μl of caspase-3 substrate (Ac-DEVD-pNA) or caspase-9 substrate (Ac-LEHD-pNA) was then incubated in 96-well plates at 37°C for 4 h. The optical density was subsequently measured at 405 nm using a microplate reader. The relative caspase activity was expressed as the percentage of enzyme activity relative to the control, as described previously [10, 32]. The experiments were repeated in triplicate.

Immunofluorescence assay

Briefly, HCC cells were fixed with 3% paraformaldehyde and permeabilized in 0.1% Triton X-100. The cells were then incubated with the appropriate primary and secondary Abs, and the DNA was stained using DAPI. The immunostained cells were photographed under an inverted fluorescence microscope.

Immunoblotting

The immunoblotting methodology has been described previously [30, 33]. In brief, protein was extracted, and the protein concentrations of cell lysates were determined using the Bio-Rad Protein Assay (Bio-Rad, Richmond, CA, USA). The lysates were then resolved by SDS/PAGE, and the proteins were transferred to polyvinylidene difluoride (PVDF) membranes. The membranes were blocked with 5% skim milk, incubated with primary Ab and subsequently incubated with alkaline phosphatase-conjugated secondary Ab, followed by detection with enhanced chemiluminescence reagent (Pierce Chemical, Rockford, IL, USA). β-actin was used as a protein loading control, and the protein levels were normalized to the β-actin band density.

Transfection of siRNAs

The siRNA transfection methods have been previously described in detail [10, 34]. Briefly, cells were grown to 60 to 70% confluence and incubated with siRNAs at a final concentration of 0.1 μM using Lipofectamine[TM] 2000 (Invitrogen, Beijing, China) in serum-free medium for 24 h. The cells were then subjected to the assays. The siRNAs produced by GenePharma (Shanghai, China) and their targeted genes are shown in Table 1.

Table 1. The siRNAs used in this study and their targeted genes.

Gene	GenBank no.	Strands	Reference
Akt	NM_001014431.1	sense strand: 5′-GUGGUCAUGUACGAGAUGATT-3′	[7]
		antisense strand: 5′-UCAUCUCGUACAUGACCACTT-3′	
CHOP	NM_001195053.1	sense strand: 5'-CCAGGAAACGGAAACAGAGTT-3'	[22]
		antisense strand: 5'-CUCUGUUUCCGUUUCCUGGTT-3'	
IRE1	NM_001433.3	sense strand: 5′-GGAAGGUGAUGCACAUCAATT-3′	[22]
		antisense strand: 5′-UUGAUGUGCAUCACCUUCCTC-3′	
eIF2α	NM_032025.3	sense strand: 5′- GGGAAGUACUCAUUAAUAATT-3′	[22]
		antisense strand: 5′- UUAUUAAUGAGUACUUCCCGT-3′	
Control	_	sense strand: 5′-UUCUCCGAACGUGUCACGU-3′	[34]
		antisense strand: 5′-ACGUGACACGUUCGGAGAA-3′	

Abbreviations: IRE1, inositol-requiring enzyme 1; eIF2, eukaryotic initiation factor 2; CHOP, C/EBP-homologous protein.

doi:10.1371/journal.pone.0138485.t001

Statistical analysis

Quantitative data are expressed as the mean ± standard deviation. Comparisons among multiple groups were performed using one-way analysis of variance (ANOVA) test followed by Dunnett's test. $P < 0.05$ was considered to indicate significant differences for all analyses.
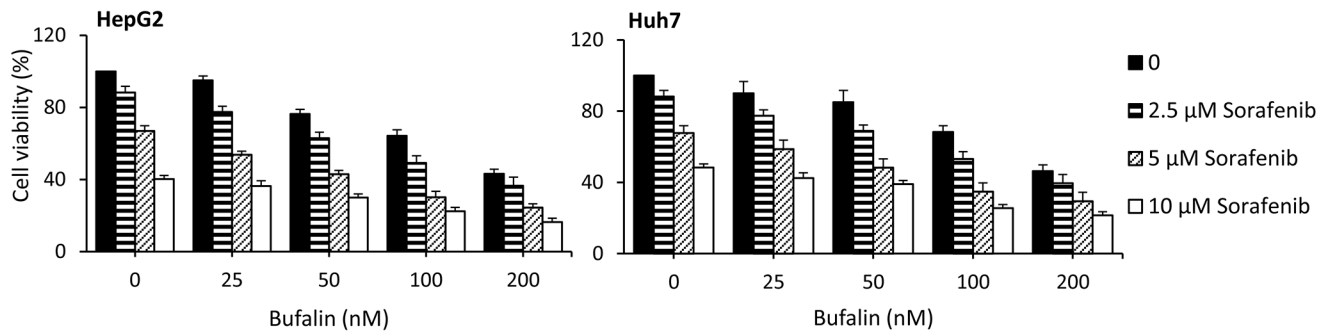
Results

Bufalin synergizes with sorafenib to inhibit HCC cell growth

To investigate the effect of bufalin in combination with sorafenib on cell growth, HepG2 and Huh7 cells were incubated with increasing concentrations of bufalin and/or sorafenib for 24, 48, or 72 h. Cell survival was then assessed via the CCK-8 assay. As shown in Fig 1A and 1B, bufalin synergized with sorafenib to inhibit cell viability in a dose- and time-dependent manner. Although 25 nM and 50 nM bufalin alone had a limited effect on the cell growth index, as previously described [23], bufalin in combination with sorafenib significantly reduced cell growth compared with bufalin or sorafenib treatment alone. Moreover, the antitumor effect of bufalin was enhanced at both 100 nM and 200 nM, which demonstrated the dose-dependent activation of bufalin in combination with sorafenib. To investigate whether the effects of bufalin and sorafenib were synergistic, we calculated the coefficient of drug interaction (CDI), as described previously [35–37]. All CDIs for the combination of bufalin and sorafenib at various concentrations were less than 1 (Fig 1A; S1 and S2 Tables), indicating that bufalin and sorafenib synergistically inhibited cell proliferation. Moreover, the combination of 100 nM bufalin and 5 μM sorafenib yielded CDIs of 0.74 and 0.70 for HepG2 and Huh7 cells, respectively. This combination optimized the synergistic effect and was consequently used in subsequent experiments.

Bufalin synergizes with sorafenib to induce apoptosis in HCC cells

To investigate the synergistic effects of bufalin and sorafenib on apoptosis, HepG2 and Huh7 cells were incubated with 100 nM bufalin and/or 5 μM sorafenib for 48 h, harvested, stained with Annexin V/PI, and then subjected to flow cytometry to determine the apoptosis rate. As shown in Fig 2A, the apoptosis rates were 6.6%, 16.8%, 15.7% and 34.9% in HepG2 cells and 4.5%, 13.1%, 12.1%, and 38.7% in Huh7 cells for the control, bufalin, sorafenib and bufalin + sorafenib groups, respectively. Additionally, the CDIs were 0.78 and 0.80 in HepG2 and
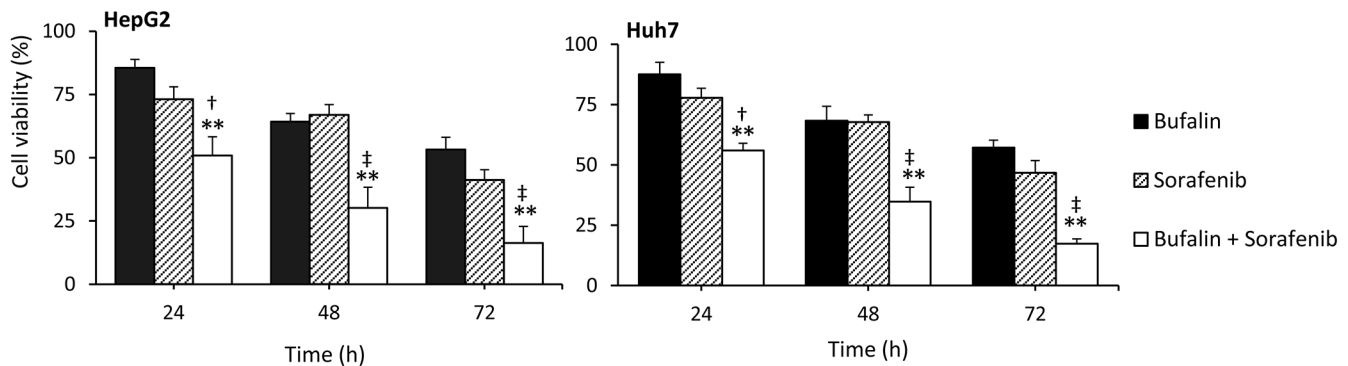
A

B

Fig 1. Bufalin synergizes with sorafenib to inhibit HCC cell growth. (A) HepG2 and Huh7 cells were exposed to different concentrations of bufalin and/or sorafenib for 48 h. (B) The above cells were incubated with 100 nM bufalin and/or 5 μM sorafenib for different periods. Cell viability (%) was then compared with the corresponding untreated cells. The data represent three independent experiments. "**" (P<0.001) vs. bufalin alone. "†" (P<0.05) and "‡" (P<0.001) vs. sorafenib alone.

doi:10.1371/journal.pone.0138485.g001

Huh7 cells, respectively, indicating that bufalin and sorafenib synergistically induced apoptosis. To confirm the ability of bufalin and sorafenib to induce apoptosis, confocal microscopy was used to view the Annexin V/PI-stained cells. As shown in Fig 2B, early-stage apoptotic cells (green fluorescent membranes) and late-stage apoptotic cells (green fluorescent membranes and nuclei) were abundant in bufalin- or sorafenib-treated cells but rare in the untreated control cells. Additionally, treatment with a combination of bufalin and sorafenib increased the number of apoptotic cells compared with bufalin or sorafenib treatment alone. Bufalin and sorafenib treatment each significantly increased the cellular activities of caspase-3 and caspase-9 compared with the activities in untreated cells, and the combination treatment further increased these activities compared with bufalin or sorafenib treatment alone (Fig 2C).

Bufalin suppresses sorafenib-induced Akt activation to reverse sorafenib resistance in HCC cells

As shown in our previous study [7, 10], increased p-Akt is responsible for resistance to sorafenib, and specific inhibition of Akt synergizes with sorafenib to inhibit the proliferation and promote the apoptosis of sorafenib-resistant cells both *in vitro* and *in vivo*. Therefore, in the current study, we examined the effect of bufalin on Akt expression. For this purpose, HCC cells
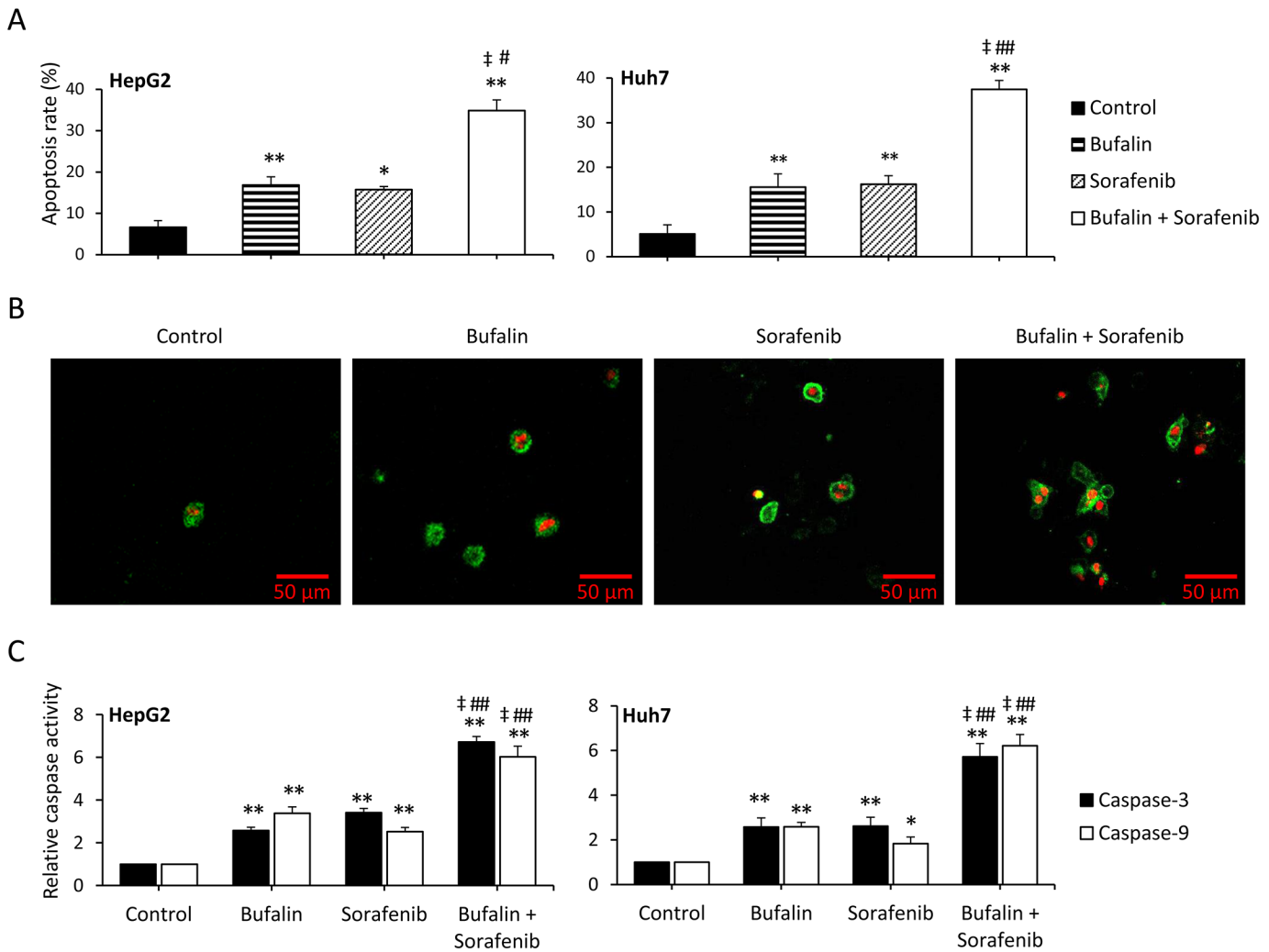
Fig 2. Bufalin synergizes with sorafenib to induce apoptosis in HCC cells. HepG2 and Huh7 cells were incubated with 100 nM bufalin and/or 5 µM sorafenib for 48 h. (A) The cells were stained with Annexin V/PI and subjected to flow cytometry to measure the apoptosis rate (%). (B) Representative images were taken of Huh7 cells stained with Annexin V/PI and viewed with a laser-scanning confocal microscope. (C) The activities of caspase-3 and caspase-9 were measured. The data represent three independent experiments. Untreated cells served as controls. "*" (P<0.05) and "**" (P<0.001) vs. untreated control; "‡" (P<0.001) vs. sorafenib alone; "#" (P<0.05) and "##" (P<0.001) vs. bufalin alone.

doi:10.1371/journal.pone.0138485.g002

were incubated with increasing concentrations of bufalin for 48 h and then subjected to an immunoblotting analysis. Bufalin downregulated the expression of p-Akt in a concentration-dependent manner but did not affect Akt expression (Fig 3A; S1A Fig), and as shown in Fig 3B and S1B Fig, sorafenib upregulated the expression of p-Akt. LY294002, a potent inhibitor of Akt, synergized with sorafenib to inhibit cell viability and promote apoptosis (S2 and S3 Figs), indicating that the sorafenib-induced activation of Akt was responsible for the resistance to sorafenib. When bufalin was combined with sorafenib, bufalin significantly suppressed sorafenib-induced Akt activation (P<0.001; Fig 3B and S1B Fig). The above results were further supported by an immunofluorescence assay (Fig 3C).

Consequently, perifosine, another specific Akt inhibitor, was used to determine the role of Akt in the synergistic effects of bufalin and sorafenib. Specifically, HepG2 and Huh7 cells were exposed to 100 nM bufalin and/or 5 µM sorafenib for 48 h in the presence or absence of perifosine. A cell viability analysis showed that perifosine significantly increased the antitumor
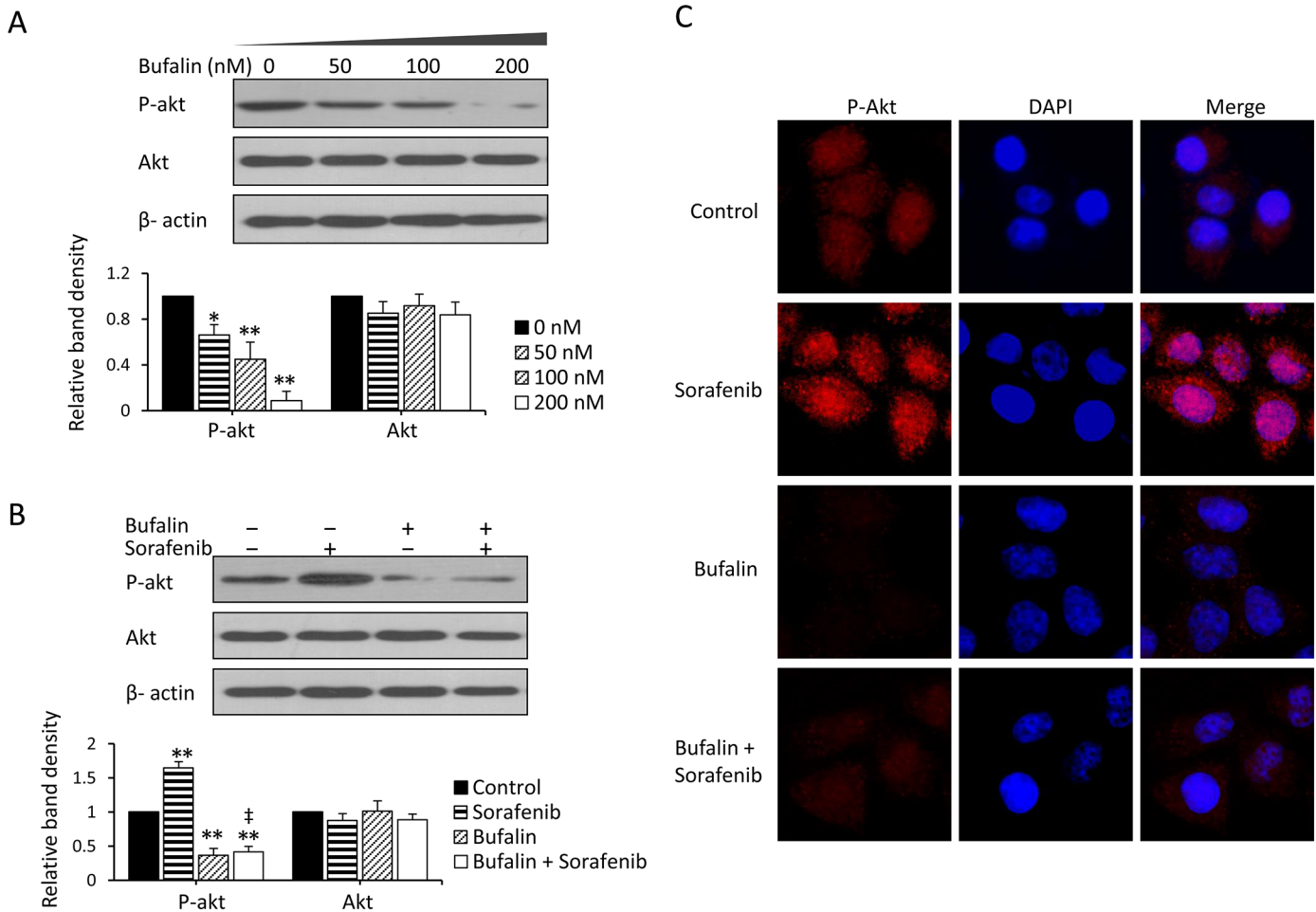
Fig 3. Bufalin suppresses sorafenib-induced Akt activation to reverse resistance to sorafenib in HCC cells. A-B, Huh7 cells were exposed to different concentrations of bufalin (A) or to 100 nM bufalin and/or 5 µM sorafenib (B) for 48 h. Untreated cells served as controls. Cell lysates were immunoblotted, and the density of each band was measured. Band densities were normalized to β-actin. The relative band density from untreated cells was defined as 1. (C) The Huh7 cells from (B) were immunostained with anti-p-Akt Ab (red) and DAPI (cellular nuclei, blue) and viewed with an inverted fluorescence microscope. The data represent three independent experiments. "*" ($P<0.05$) and "**" ($P<0.001$) vs. untreated control; "‡" ($P<0.001$) vs. sorafenib alone.

doi:10.1371/journal.pone.0138485.g003

activity of sorafenib by inhibiting cell growth and inducing apoptosis in both the presence and the absence of bufalin (Fig 4A and 4B). We next examined whether depletion of Akt by siRNAs could potentiate the anticancer activities of bufalin in combination with sorafenib in HCC. HepG2 and Huh7 cells were transfected with control or Akt siRNA for 24 h and then further incubated for 24 h with 100 nM bufalin, 5 µM sorafenib or a combination of these two drugs. As shown in Fig 4C and 4D, the depletion of Akt by siRNA increased the antitumor activity of sorafenib when combined with bufalin by inhibiting cell growth and inducing apoptosis. This finding indicated that bufalin suppresses sorafenib-induced Akt activation, reversing sorafenib resistance in HCC cells.

Bufalin-induced Akt inactivation is IRE1 dependent

As shown in our previous study [23], ER stress is involved in the antitumor activities of bufalin. To investigate the role of ER stress in bufalin-induced Akt inactivation, Huh7 cells were incubated with 100 nM bufalin for 0, 12, 24, or 48 h and then subjected to immunoblotting. The
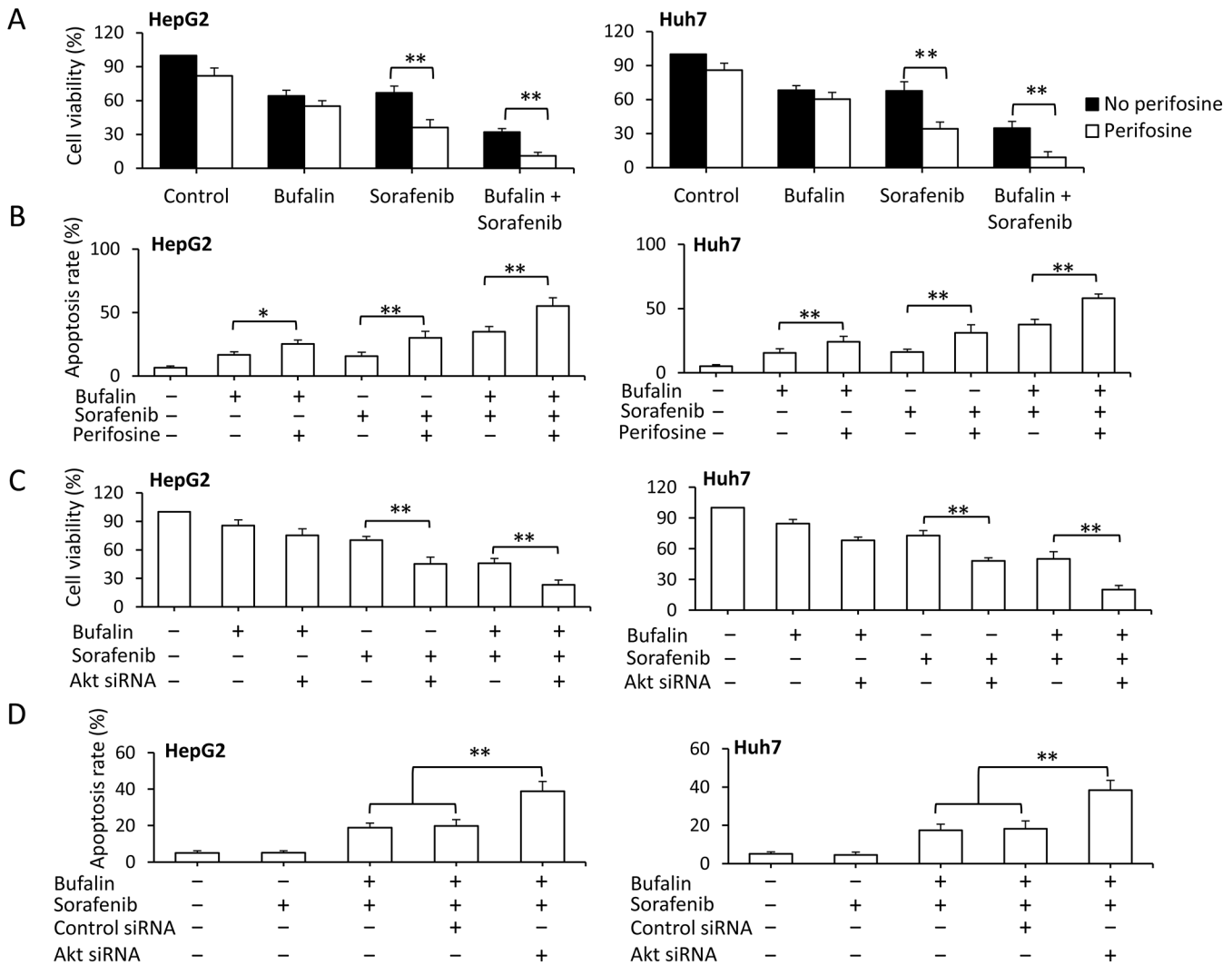
Fig 4. Inhibition of Akt enhances sorafenib-induced growth inhibition and apoptosis. A-B, HepG2 and Huh7 cells were exposed to 100 nM bufalin and/ or 5 µM of sorafenib in the presence or absence of perifosine (10 µM) for 48 h. (A) Cell viability (%) was then compared with the corresponding untreated cells. (B) The percentages of apoptotic cells (%) were measured by flow cytometry. Untransfected cells served as controls. C-D, HepG2 and Huh7 cells were transfected with control or Akt siRNA for 24 h and then incubated with 100 nM bufalin, 5 µM sorafenib, or a combination of the two drugs for 24 h. (C) Cell viability (%) was compared with control siRNA-transfected cells. (D) The percentages of apoptotic cells (%) were measured by flow cytometry. Untransfected cells served as controls. The data represent three independent experiments. "**" represents P<0.001.

doi:10.1371/journal.pone.0138485.g004

protein expression levels of eIF2α, CHOP, and IRE1, the key molecules involved in ER stress, were detected. As shown in Fig 5A, bufalin time-dependently upregulated the expression of eIF2α, CHOP, and IRE1. These results indicate that the three major branches of the UPR are activated in response to ER stress. Moreover, the effect of bufalin on eIF2α, CHOP, and IRE1 expression negatively correlates with p-Akt expression (Fig 3A).

ER stress was recently reported to negatively regulate the AKT/mTOR pathway [38]. We also previously reported that the effects of eIF2α, CHOP, and IRE1 on apoptosis and autophagy are discrepant [23]. Thus, we hypothesized that bufalin-induced Akt inactivation is ER stress dependent. To verify this hypothesis, we used siRNA to knock down the expression of eIF2α, CHOP, or IRE1. In particular, Huh7 cells were transfected with control, eIF2α, CHOP, or IRE1 siRNA for 24 h, followed by further incubation for 24 h with 100 nM bufalin and
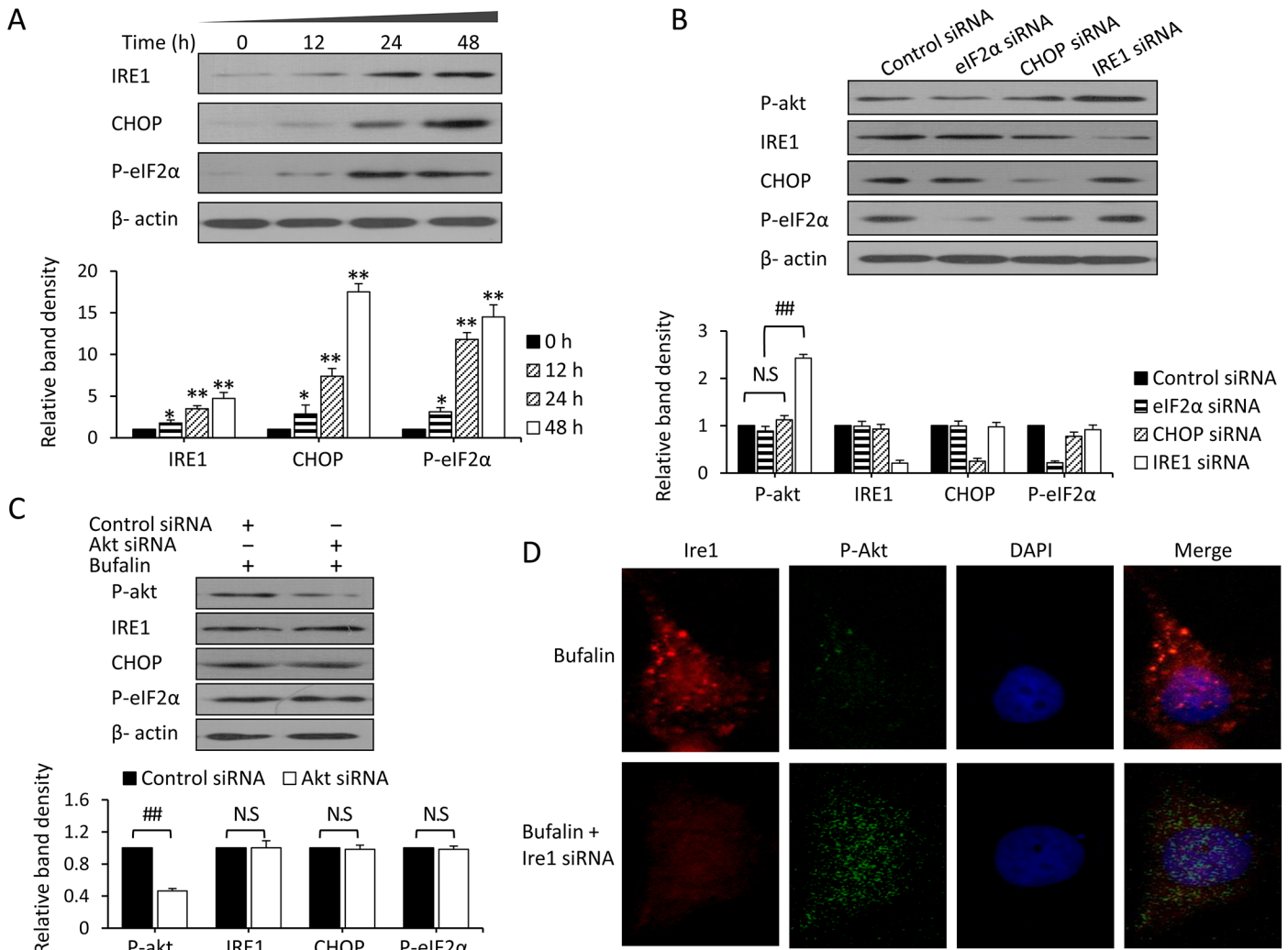
Fig 5. Bufalin-induced Akt inactivation is IRE1 dependent. (A) Huh7 cells were exposed to 100 nM bufalin for 12, 24, or 48 h. Untreated cells served as controls. Cell lysates were immunoblotted, and the density of each band was measured. Band densities were normalized to β-actin. (B) Huh7 cells were transfected with control, eIF2α, CHOP, or IRE1 siRNA for 24 h and then incubated with 100 nM bufalin for 24 h. Cell lysates were immunoblotted, and the density of each band was measured. Band densities were normalized to β-actin. The relative band density from control-siRNA transfected cells was defined as 1. (C) Huh7 cells were transfected with control or Akt siRNA for 24 h and then incubated with 100 nM bufalin for 24 h. Cell lysates were immunoblotted, and the density of each band was measured. Band densities were normalized to β-actin. The relative band density from control-siRNA transfected cells was defined as 1. (D) Huh7 cells were incubated with 100 nM bufalin and/or 5 μM sorafenib for 48 h. The cells were immunostained with Abs against IRE1 (red) and p-Akt (green) as well as with DAPI (cellular nuclei, blue). The data represent three independent experiments. N.S., not significant. "*" (P<0.05) and "**" (P<0.001) vs. untreated control; "##" represents P<0.001.

doi:10.1371/journal.pone.0138485.g005

subsequent immunoblotting. As shown in Fig 5B, the silencing of IRE1 by siRNA reversed the bufalin-induced p-Akt downregulation and significantly increased the expression of p-Akt protein, but the silencing of eIF2α or CHOP did not affect p-Akt expression. Next, Akt siRNA was used to silence Akt, and eIF2α, CHOP, and IRE1 expression was detected by immunoblotting. As shown in Fig 5C, the silencing of Akt by siRNA significantly downregulated the expression of p-Akt protein but did not affect eIF2α, CHOP, or IRE1 expression. Moreover, silencing IRE1 with siRNA in HepG2 cells reversed bufalin-induced p-Akt downregulation, but Akt siRNA did not affect IRE1 expression (S4 Fig). The immunofluorescence staining results revealed that silencing IRE1 with siRNA reversed the bufalin-induced p-Akt downregulation

(Fig 5D). When IRE1 was depleted by IRE1 siRNA, inhibition of proliferation and stimulation of apoptosis by bufalin alone or in combination with sorafenib were blocked (S5 Fig). These results indicate that bufalin-induced p-Akt downregulation is related to ER stress and depends on IRE1.

Bufalin reverses acquired resistance to sorafenib by downregulating p-Akt via IRE1 activation

To examine the role of bufalin in reversing acquired resistance to sorafenib, we continuously exposed Huh7 and HepG2 cells to gradually increasing concentrations of sorafenib. After several months of culture, sorafenib-resistant Huh7-Sora and HepG2-Sora cells were established. As showed in Fig 6A, Huh7-Sora recovered a proliferative capacity comparable to that of the corresponding parental cells. To investigate the sorafenib-resistant characteristics of Huh7-Sora cells, the Huh7-Sora and corresponding parental cells were exposed to increasing concentrations of sorafenib for 48 h, and the cell viability was then detected. As shown in Fig 6B, the cell viability of Huh7-Sora cells was significantly higher than that of Huh7 cells. Even at 15 mmol/L sorafenib, the viability of Huh7-Sora remained at 65.6%, whereas most Huh7 cells had died (15.6%). This finding indicates that Huh7-Sora cells were less sensitive to sorafenib than their parental counterparts were. We then examined the antitumor activity of bufalin in sorafenib-resistant cells. We observed that Huh7-Sora cells were more sensitive to the growth-inhibitory effects of bufalin than their control counterparts were (IC50 55.85±0.6 nM vs. 179.75±1.3 nM; Fig 6C). The HepG2-Sora cells also recovered their proliferative capacity and showed decreased sensitivity to sorafenib, accompanied by an increased sensitivity to bufalin that was comparable to that of the parental cells (S6 Fig).

Based on the above results, we investigated whether the ability of bufalin to activate ER stress and inhibit Akt activation was responsible for the increased sensitivity to bufalin in the sorafenib-resistant cells. We first detected the protein expression of Akt in Huh7 and Huh7-Sora cells. As shown in Fig 6D, p-Akt was significantly upregulated in Huh7-Sora cells compared with Huh7 cells, whereas the difference in Akt expression was not significant between these two cell types. We then incubated control siRNA- or IRE1 siRNA-transfected Huh7-Sora cells with sorafenib for 24 h and examined p-Akt and IRE1 expression. Bufalin upregulated the expression of IRE1 and downregulated p-Akt in control siRNA-transfected cells (Fig 6E). However, when IRE1 was depleted by IRE1 siRNA, bufalin-induced p-Akt downregulation was blocked in Huh7-Sora cells, and p-Akt was upregulated (Fig 6E). The silencing of IRE1 by siRNA inhibited the antitumor activity of bufalin both alone and in combination with sorafenib due to pro-proliferation and anti-apoptosis effects (S7 Fig). These results indicate that bufalin reverses acquired resistance to sorafenib by downregulating p-Akt via IRE1 activation.

Discussion

Although sorafenib represents the standard first-line systemic treatment for advanced HCC, drug resistance to sorafenib, which is characterized by a low partial response rate to sorafenib, is a unique concern due to the shortage of alternative systemic treatments for HCC [4, 39]. The present study has demonstrated that bufalin, an ingredient of the traditional Chinese medicine *Chan su* that has been approved to treat tumor patients, synergizes with sorafenib to suppress the growth of HCC cells both *in vitro* and *in vivo*. The synergistic effect of these two agents is primarily due to the ability of bufalin to mitigate the sorafenib-induced activation of Akt, which contributes to the resistance of HCC cells to sorafenib. Furthermore, both of these drugs can individually inhibit the proliferation of HCC cells and induce apoptosis. Moreover, the bufalin-induced p-Akt downregulation depends on ER stress and is mediated by the IRE1
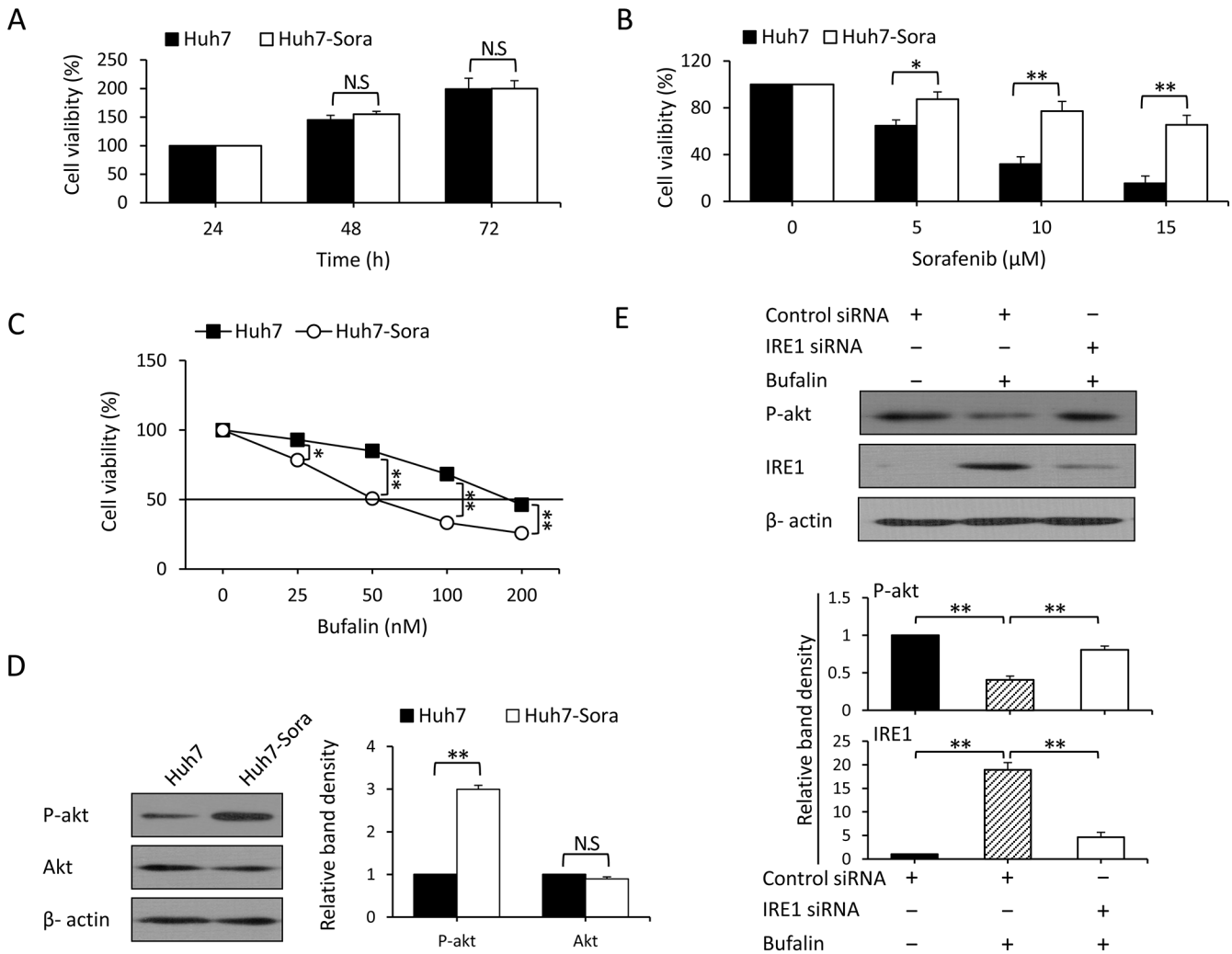
Fig 6. Bufalin reverses acquired resistance to sorafenib by downregulating p-Akt via IRE1 activation. (A) Huh7 and Huh7-Sora cells were cultured in complete medium, and the viability was examined after 24, 48, and 72 h in culture. (B) The above cells were exposed to increasing concentrations of sorafenib for 48 h. Untreated cells served as controls. Cell viability (%) was compared to the corresponding untreated cells. (C) The above cells were exposed to increasing concentrations of bufalin for 48 h. Untreated cells served as controls. Cell viability (%) was compared with the corresponding untreated cells. The black line indicates the IC50. (D) The lysates of cells from (A) were subjected to immunoblotting. Band densities were normalized to β-actin. The relative band density from Huh7 cells was defined as 1. (E) Huh7-Sora cells were transfected with control or IRE1 siRNA for 24 h and then incubated with 100 nM bufalin for 24 h. Cell lysates were immunoblotted, and the density of each band was measured. Band densities were normalized to β-actin. The relative band density from control cells was defined as 1. The data represent three independent experiments. N.S., not significant. "*" represents P<0.05, "**" represents P<0.001.

doi:10.1371/journal.pone.0138485.g006

pathway. This mechanism is also involved in the ability of bufalin to reverse sorafenib resistance. The encouraging results presented herein warrant future investigation of the use of bufalin as an HCC treatment, especially in combination with sorafenib.

The PI3K/Akt pathway is involved in the development and progression of HCC and is activated in 92.3% of HCC specimens [5, 6]. Therefore, this pathway is a key target of HCC treatment. Sorafenib was previously reported to activate the PI3K/Akt pathway, and blocking the PI3K/Akt signaling pathway enhances the efficacy of sorafenib [8, 10, 40, 41]. In a previous report, we showed that sustained sorafenib treatment could activate Akt in both human HCC patients and mouse HCC models [7]. Here, we showed that sorafenib activated Akt in both parental and sorafenib-resistant HCC cells. The PI3K/Akt pathway includes over one hundred

molecules and interacts with tumor-associated pathways, such as those involved in cell growth, invasion, metastasis, apoptosis, and autophagy, among other pathways [7]. Therefore, in the present study, blocking Akt with a specific inhibitor, such as siRNA or bufalin, in combination with sorafenib synergistically inhibited cell growth and induced apoptosis by deregulating downstream factors in HCC cells to reverse both inherent and acquired resistance to sorafenib. This finding is in agreement with the results of our previous report [7, 10].

ER stress is a cellular stress response mediated by the UPR, which is activated by different stimuli, including chemotherapy drugs. The effect of ER stress on tumor cells is pleiotropic and involves pro-survival or pro-apoptotic signals [21–23, 42]. When ER stress is extensive or sustained, the function of the ER cannot be restored, leading to caspase-dependent cell death [43]. Therefore, ER stress is involved in the antitumor activities of numerous chemotherapy drugs for HCC [16, 22], breast cancer [18], ovarian cancer [17], and nasopharyngeal tumors [44], among other cancers. However, the role of ER stress in chemotherapy resistance in HCC [16], breast cancer [18, 45], and ovarian cancer [17] remains controversial. Certain research has shown that ER stress induces drug resistance and that inhibition of ER stress reverses drug resistance [14–16]. Other research has shown that ER stress is responsible for the sensitivity of cancer cells to chemotherapy drugs [45] and that inducing ER-stress-associated apoptosis reverses drug resistance [46, 47]. Moreover, the inability of anticancer drugs to induce ER stress is responsible for acquired resistance to chemotherapy in human laryngeal carcinoma cells [20]. Sorafenib-induced ER-stress-related apoptosis has also been reported in HCC [22, 24]. Here, we showed that bufalin-induced ER stress activation synergistically enhanced the antitumor activity of sorafenib in parental cells and reversed acquired sorafenib resistance in sorafenib-resistant HCC cells. However, we did not investigate the effect of sorafenib on ER stress in the drug resistance model. Nevertheless, the above results at least partly support the idea that ER stress may also be involved in acquired drug resistance to sorafenib because sustained drug exposure could induce an adaptive response consisting of downregulation of sorafenib-induced ER stress, inhibition of apoptosis pathways and activation of compensatory pro-survival signals. Generally, ER-stress-induced apoptosis depends on caspase-4 and caspase-9, but the roles of caspase-3 and caspase-9 have not yet been reported [23, 48]. Cross-talk between ER stress signals and cell death signals, such as PI3K/Akt, Raf/MAPK/ERK, and autophagy, has also been observed [22, 23, 49]. ER stress was recently reported to negatively regulate p-Akt expression [38] and to activate Akt [15] as well. One report also showed that PI3K/Akt inactivation could mediate ER-stress-induced ERK activation [43]. Therefore, the complex effect of ER stress on the PI3K/Akt pathway in sorafenib resistance remains unclear. Here, we showed that bufalin downregulated p-Akt in parental and sorafenib-resistant HCC cells in an ER-stress-dependent manner. However, the roles of the three main downstream effectors of ER stress in the induction of cell death differ [22, 38], which is in agreement with our previous report [23]. To investigate whether the roles of IRE1, eIF2α, and ATF6 are different, IRE1 and eIF2α were directly knocked out with IRE1 and eIF2α siRNAs, respectively, and siRNA was also used to block CHOP, the downstream cofactor of eIF2α and ATF6. Our novel results indicate that ER-stress-induced p-Akt inactivation is IRE1 dependent but independent of eIF2α and ATF6.

Bufalin, the digoxin-like primary component of the traditional Chinese medicine *Chan su*, was initially identified more than 1000 years ago in extracts from the skin and parotid venom glands of *Bufo bufo gargarizans Cantor*. This drug has a broad spectrum of biological activities, including cardiotonic, anesthetic, blood pressure stimulatory, and respiratory effects [26, 50]. In modern Chinese medical practice, the drug has been widely used in clinical trials to treat various intermediate and advanced solid tumors due to its antitumor activity [23, 25, 49, 51, 52]. Recently, bufalin has garnered increasing attention due to its ability to inhibit cell growth and induce apoptosis in HCC cells and animal models of HCC, a cancer that is notoriously

inherently resistant to systemic chemotherapy [26–28, 51, 53, 54]. However, the antitumor mechanism of bufalin is complex and controversial. Bufalin has been reported to increase the expression of p-Akt in HCC cells at concentrations of 50 nM and 250 nM [49]. However, at the routine concentration of 100 nM [26–28] and at the low level of 10 nM [53], bufalin consistently downregulated p-Akt expression. Here, we have demonstrated that bufalin dose-dependently downregulated p-Akt expression, which is in accordance with previous reports [26, 27]. Recently, bufalin was also reported to reverse resistance to 5-fluorouracil and doxorubicin in HCC [52, 55]. Moreover, bufalin could enhance the anti-proliferative effects of sorafenib in HCC cells [49]. The antitumor activity of bufalin has been attributed to its ability to induce ER stress [56], which is in agreement with our previous report [23]. Here, we specifically reported that bufalin-induced p-Akt downregulation was ER stress dependent and mediated by the IRE1 pathway. Bufalin also reversed acquired resistance to sorafenib via this pathway.

In summary, the present study demonstrated that bufalin reversed both inherent and acquired resistance to sorafenib in HCC cells by suppressing sorafenib-mediated Akt activation. This effect may be due to bufalin-induced ER stress, which subsequently downregulated p-Akt, inhibited cell growth and induced apoptosis. Moreover, this activity depended on the IRE1 pathway. Although the latent mechanism by which bufalin reverses resistance to sorafenib is complex and unclear, the ER stress pathway engages in cross-talk with many pathways related to cell growth and apoptosis. We showed that the bufalin-induced inactivation of Akt at least partly depended on ER stress and was mediated by the IRE1 pathway. These results warrant further studies of the utility of bufalin alone or in combination with sorafenib as a first- or second-line treatment after sorafenib failure for advanced HCC.

Supporting Information

S1 Fig. Bufalin suppresses sorafenib-induced Akt activation in HCC cells. A-B, HepG2 cells were exposed to increasing concentrations of bufalin (A) or to 100 nM bufalin and/or 5 μM sorafenib (B) for 48 h and then subjected to immunoblotting. Band densities were normalized to β-actin. The relative band density from untreated cells was defined as 1. The data represent three independent experiments. "**" (P<0.001) vs. untreated control; "‡" (P<0.001) vs. sorafenib alone; "#" (P<0.05) and "##" (P<0.001) vs. bufalin alone.
(TIF)

S2 Fig. Inhibition of Akt enhances sorafenib-induced growth inhibition. HepG2 (A) and Huh7 (B) cells were incubated with 10 mM LY294002, 5 μM sorafenib, or a combination of the two drugs for 48 h. Untransfected cells served as controls. Cell viability (%) was compared with the corresponding untreated cells. The data represent three independent experiments. "*" (P<0.05) and "**" (P<0.001) vs. untreated control; "‡" (P<0.001) vs. sorafenib alone; "##" (P<0.001) vs. LY294002 alone.
(TIF)

S3 Fig. Inhibition of Akt enhances sorafenib-induced apoptosis. HepG2 (A) and Huh7 (B) cells were incubated with 10 mM LY294002, 5 μM sorafenib, or a combination of the two drugs for 48 h. Untransfected cells served as controls. The cells were analyzed using flow cytometry to detect apoptosis. The data represent three independent experiments. "*" (P<0.05) and "**" (P<0.001) vs. untreated control; "‡" (P<0.001) vs. sorafenib alone; "##" (P<0.001) vs. LY294002 alone.
(TIF)

S4 Fig. Bufalin-induced Akt inactivation is IRE1 dependent. A-B, HepG2 cells were transfected with control, Akt or IRE1 siRNA for 24 h and then incubated with or without 100 nM

bufalin for 24 h. Cell lysates were immunoblotted, and representative bands are shown (A). (B) The density of each band in (A) was measured and normalized to β-actin. The data represent three independent experiments. N.S., not significant. "**" represents P<0.001.
(TIF)

S5 Fig. Silencing of IRE1 by siRNA inhibits the antitumor activity of bufalin in Huh7 cells. A-B, Huh7 cells were transfected with control or IRE1 siRNA for 24 h and then incubated with 100 nM bufalin, 5 μM sorafenib, or a combination of the two drugs for 48 h. (A) Cell viability (%) was measured. (B) The percentages of apoptotic cells (%) were measured by flow cytometry. Control siRNA-transfected cells served as controls. The relative band density from control cells was defined as 1. The data represent three independent experiments. "*" represents P<0.05, "**" represents P<0.001.
(TIF)

S6 Fig. Sorafenib-resistant HCC cells display increased sensitivity to bufalin. (A) HepG2 and HepG2-Sora cells were cultured in complete medium, and the viability was examined after 24, 48, and 72 h in culture. (B) The above cells were exposed to increasing concentrations of sorafenib for 48 h. Untreated cells served as controls. Cell viability (%) was compared with the corresponding untreated cells. (C) The above cells were exposed to increasing concentrations of bufalin for 48 h. Untreated cells served as controls. Cell viability (%) was compared with to the corresponding untreated cells. The data represent three independent experiments. N.S., not significant. The black line indicates the IC50. "*" represents P<0.05, "**" represents P<0.001.
(TIF)

S7 Fig. Silencing of IRE1 by siRNA inhibits the antitumor activity of bufalin in Huh7-Sora cells. A-B, Huh7-Sora cells were transfected with control or IRE1 siRNA for 24 h and then incubated with 50 nM bufalin, 10 μM sorafenib, or a combination of the two drugs for 48 h. (A) Cell viability (%) was measured. (B) The percentages of apoptotic cells (%) were measured by flow cytometry. Control siRNA-transfected cells served as controls. The data represent three independent experiments. "**" represents P<0.001.
(TIF)

S1 Table. The CDIs of bufalin in combination with sorafenib in HepG2 cells.
(DOCX)

S2 Table. The CDIs of bufalin in combination with sorafenib in Huh7 cells.
(DOCX)

Acknowledgments

Author Contributions

Conceived and designed the experiments: BZ XS LX. Performed the experiments: BZ FH HY DZ XJ TF SP. Analyzed the data: FH HY DZ XJ TF LX. Contributed reagents/materials/analysis tools: BZ FH SP LX. Wrote the paper: BZ FH LX.

References

1. Torre LA, Bray F, Siegel RL, Ferlay J, Lortet-Tieulent J, Jemal A. Global cancer statistics, 2012. CA: a cancer journal for clinicians. 2015; 65(2):87–108.

2. Zhu AX. Systemic treatment of hepatocellular carcinoma: dawn of a new era? Annals of surgical oncology. 2010; 17(5):1247–56. doi: 10.1245/s10434-010-0975-6 PMID: 20405329

3. Llovet JM, Ricci S, Mazzaferro V, Hilgard P, Gane E, Blanc JF, et al. Sorafenib in advanced hepatocellular carcinoma. The New England journal of medicine. 2008; 359(4):378–90. doi: 10.1056/NEJMoa0708857 PMID: 18650514

4. Zhai B, Sun XY. Mechanisms of resistance to sorafenib and the corresponding strategies in hepatocellular carcinoma. World journal of hepatology. 2013; 5(7):345–52. doi: 10.4254/wjh.v5.i7.345 PMID: 23898367

5. Mendoza MC, Er EE, Blenis J. The Ras-ERK and PI3K-mTOR pathways: cross-talk and compensation. Trends in biochemical sciences. 2011; 36(6):320–8. doi: 10.1016/j.tibs.2011.03.006 PMID: 21531565

6. Zhou L, Huang Y, Li J, Wang Z. The mTOR pathway is associated with the poor prognosis of human hepatocellular carcinoma. Med Oncol. 2010; 27(2):255–61. doi: 10.1007/s12032-009-9201-4 PMID: 19301157

7. Zhai B, Hu F, Jiang X, Xu J, Zhao D, Liu B, et al. Inhibition of Akt reverses the acquired resistance to sorafenib by switching protective autophagy to autophagic cell death in hepatocellular carcinoma. Molecular cancer therapeutics. 2014; 13(6):1589–98. doi: 10.1158/1535-7163.MCT-13-1043 PMID: 24705351

8. Gedaly R, Angulo P, Hundley J, Daily MF, Chen C, Koch A, et al. PI-103 and sorafenib inhibit hepatocellular carcinoma cell proliferation by blocking Ras/Raf/MAPK and PI3K/AKT/mTOR pathways. Anticancer research. 2010; 30(12):4951–8. PMID: 21187475

9. Chen KF, Chen HL, Tai WT, Feng WC, Hsu CH, Chen PJ, et al. Activation of phosphatidylinositol 3-kinase/Akt signaling pathway mediates acquired resistance to sorafenib in hepatocellular carcinoma cells. The Journal of pharmacology and experimental therapeutics. 2011; 337(1):155–61. doi: 10.1124/jpet.110.175786 PMID: 21205925

10. Zhai B, Jiang X, He C, Zhao D, Ma L, Xu L, et al. Arsenic trioxide potentiates the anti-cancer activities of sorafenib against hepatocellular carcinoma by inhibiting Akt activation. Tumour biology: the journal of the International Society for Oncodevelopmental Biology and Medicine. 2015; 36(4):2323–34.

11. van Malenstein H, Dekervel J, Verslype C, Van Cutsem E, Windmolders P, Nevens F, et al. Long-term exposure to sorafenib of liver cancer cells induces resistance with epithelial-to-mesenchymal transition, increased invasion and risk of rebound growth. Cancer letters. 2013; 329(1):74–83. doi: 10.1016/j.canlet.2012.10.021 PMID: 23111106

12. Lackner MR, Wilson TR, Settleman J. Mechanisms of acquired resistance to targeted cancer therapies. Future Oncol. 2012; 8(8):999–1014. doi: 10.2217/fon.12.86 PMID: 22894672

13. Bottsford-Miller JN, Coleman RL, Sood AK. Resistance and escape from antiangiogenesis therapy: clinical implications and future strategies. Journal of clinical oncology: official journal of the American Society of Clinical Oncology. 2012; 30(32):4026–34.

14. Fan L, Sun G, Ma T, Zhong F, Lei Y, Li X, et al. Melatonin reverses tunicamycin-induced endoplasmic reticulum stress in human hepatocellular carcinoma cells and improves cytotoxic response to doxorubicin by increasing CHOP and decreasing survivin. Journal of pineal research. 2013; 55(2):184–94. doi: 10.1111/jpi.12061 PMID: 23711089

15. Jiang CC, Yang F, Thorne RF, Zhu BK, Hersey P, Zhang XD. Human melanoma cells under endoplasmic reticulum stress acquire resistance to microtubule-targeting drugs through XBP-1-mediated activation of Akt. Neoplasia. 2009; 11(5):436–47. PMID: 19412428

16. Fan L, Song B, Sun G, Ma T, Zhong F, Wei W. Endoplasmic reticulum stress-induced resistance to doxorubicin is reversed by paeonol treatment in human hepatocellular carcinoma cells. PloS one. 2013; 8(5):e62627. doi: 10.1371/journal.pone.0062627 PMID: 23658755

17. Liu N, Xu Y, Sun JT, Su J, Xiang XY, Yi HW, et al. The BH3 mimetic S1 induces endoplasmic reticulum stress-associated apoptosis in cisplatin-resistant human ovarian cancer cells although it activates autophagy. Oncology reports. 2013; 30(6):2677–84. doi: 10.3892/or.2013.2771 PMID: 24100381

18. McCloy RA, Shelley EJ, Roberts CG, Boslem E, Biden TJ, Nicholson RI, et al. Role of endoplasmic reticulum stress induction by the plant toxin, persin, in overcoming resistance to the apoptotic effects of tamoxifen in human breast cancer cells. British journal of cancer. 2013; 109(12):3034–41. doi: 10.1038/bjc.2013.693 PMID: 24178758

19. Holz MS, Janning A, Renne C, Gattenlohner S, Spieker T, Brauninger A. Induction of endoplasmic reticulum stress by sorafenib and activation of NF-kappaB by lestaurtinib as a novel resistance mechanism in Hodgkin lymphoma cell lines. Molecular cancer therapeutics. 2013; 12(2):173–83. doi: 10.1158/1535-7163.MCT-12-0532 PMID: 23243060

20. Brozovic A, Vukovic L, Polancac DS, Arany I, Koberle B, Fritz G, et al. Endoplasmic reticulum stress is involved in the response of human laryngeal carcinoma cells to Carboplatin but is absent in Carboplatin-resistant cells. PloS one. 2013; 8(9):e76397. doi: 10.1371/journal.pone.0076397 PMID: 24086737

21. Kato H, Nishitoh H. Stress responses from the endoplasmic reticulum in cancer. Frontiers in oncology. 2015; 5:93. doi: 10.3389/fonc.2015.00093 PMID: 25941664

22. Shi YH, Ding ZB, Zhou J, Hui B, Shi GM, Ke AW, et al. Targeting autophagy enhances sorafenib lethality for hepatocellular carcinoma via ER stress-related apoptosis. Autophagy. 2011; 7(10):1159–72. doi: 10.4161/auto.7.10.16818 PMID: 21691147

23. Hu F, Han J, Zhai B, Ming X, Zhuang L, Liu Y, et al. Blocking autophagy enhances the apoptosis effect of bufalin on human hepatocellular carcinoma cells through endoplasmic reticulum stress and JNK activation. Apoptosis: an international journal on programmed cell death. 2014; 19(1):210–23.

24. Yi P, Higa A, Taouji S, Bexiga MG, Marza E, Arma D, et al. Sorafenib-mediated targeting of the AAA(+) ATPase p97/VCP leads to disruption of the secretory pathway, endoplasmic reticulum stress, and hepatocellular cancer cell death. Molecular cancer therapeutics. 2012; 11(12):2610–20. doi: 10.1158/1535-7163.MCT-12-0516 PMID: 23041544

25. Meng Z, Yang P, Shen Y, Bei W, Zhang Y, Ge Y, et al. Pilot study of huachansu in patients with hepatocellular carcinoma, nonsmall-cell lung cancer, or pancreatic cancer. Cancer. 2009; 115(22):5309–18. doi: 10.1002/cncr.24602 PMID: 19701908

26. Qiu DZ, Zhang ZJ, Wu WZ, Yang YK. Bufalin, a component in Chansu, inhibits proliferation and invasion of hepatocellular carcinoma cells. BMC complementary and alternative medicine. 2013; 13:185. doi: 10.1186/1472-6882-13-185 PMID: 23870199

27. Tsai SC, Yang JS, Peng SF, Lu CC, Chiang JH, Chung JG, et al. Bufalin increases sensitivity to AKT/mTOR-induced autophagic cell death in SK-HEP-1 human hepatocellular carcinoma cells. International journal of oncology. 2012; 41(4):1431–42. doi: 10.3892/ijo.2012.1579 PMID: 22858649

28. Zhang ZJ, Yang YK, Wu WZ. Bufalin attenuates the stage and metastatic potential of hepatocellular carcinoma in nude mice. Journal of translational medicine. 2014; 12:57. doi: 10.1186/1479-5876-12-57 PMID: 24581171

29. Wang J, Ma Y, Jiang H, Zhu H, Liu L, Sun B, et al. Overexpression of von Hippel-Lindau protein synergizes with doxorubicin to suppress hepatocellular carcinoma in mice. Journal of hepatology. 2011; 55(2):359–68. doi: 10.1016/j.jhep.2010.10.043 PMID: 21168458

30. Sun XP, Dong X, Lin L, Jiang X, Wei Z, Zhai B, et al. Up-regulation of survivin by AKT and hypoxia-inducible factor 1alpha contributes to cisplatin resistance in gastric cancer. The FEBS journal. 2014; 281(1):115–28. doi: 10.1111/febs.12577 PMID: 24165223

31. Xiu P, Dong X, Xu Z, Zhu H, Liu F, Wei Z, et al. Secretory clusterin contributes to oxaliplatin resistance by activating Akt pathway in hepatocellular carcinoma. Cancer science. 2013; 104(3):375–82. doi: 10.1111/cas.12088 PMID: 23279642

32. Wei Z, Jiang X, Liu F, Qiao H, Zhou B, Zhai B, et al. Downregulation of Skp2 inhibits the growth and metastasis of gastric cancer cells in vitro and in vivo. Tumour biology: the journal of the International Society for Oncodevelopmental Biology and Medicine. 2013; 34(1):181–92.

33. Dong X, Li R, Xiu P, Xu Z, Zhai B, Liu F, et al. Meloxicam executes its antitumor effects against hepatocellular carcinoma in COX-2- dependent and-independent pathways. PloS one. 2014; 9(3):e92864. doi: 10.1371/journal.pone.0092864 PMID: 24675684

34. Zhao D, Zhai B, He C, Tan G, Jiang X, Pan S, et al. Upregulation of HIF-2alpha induced by sorafenib contributes to the resistance by activating the TGF-alpha/EGFR pathway in hepatocellular carcinoma cells. Cellular signalling. 2014; 26(5):1030–9. doi: 10.1016/j.cellsig.2014.01.026 PMID: 24486412

35. Jiang H, Ma Y, Chen X, Pan S, Sun B, Krissansen GW, et al. Genistein synergizes with arsenic trioxide to suppress human hepatocellular carcinoma. Cancer science. 2010; 101(4):975–83. doi: 10.1111/j.1349-7006.2009.01464.x PMID: 20219070

36. Ma Y, Wang J, Liu L, Zhu H, Chen X, Pan S, et al. Genistein potentiates the effect of arsenic trioxide against human hepatocellular carcinoma: role of Akt and nuclear factor-kappaB. Cancer letters. 2011; 301(1):75–84. doi: 10.1016/j.canlet.2010.10.022 PMID: 21078540

37. He C, Sun XP, Qiao H, Jiang X, Wang D, Jin X, et al. Downregulating hypoxia-inducible factor-2alpha improves the efficacy of doxorubicin in the treatment of hepatocellular carcinoma. Cancer science. 2012; 103(3):528–34. doi: 10.1111/j.1349-7006.2011.02177.x PMID: 22145922

38. Qin L, Wang Z, Tao L, Wang Y. ER stress negatively regulates AKT/TSC/mTOR pathway to enhance autophagy. Autophagy. 2010; 6(2):239–47. PMID: 20104019

39. Santoro A, Rimassa L, Borbath I, Daniele B, Salvagni S, Van Laethem JL, et al. Tivantinib for second-line treatment of advanced hepatocellular carcinoma: a randomised, placebo-controlled phase 2 study. The Lancet Oncology. 2013; 14(1):55–63. doi: 10.1016/S1470-2045(12)70490-4 PMID: 23182627

40. Huynh H, Ngo VC, Koong HN, Poon D, Choo SP, Thng CH, et al. Sorafenib and rapamycin induce growth suppression in mouse models of hepatocellular carcinoma. Journal of cellular and molecular medicine. 2009; 13(8B):2673–83. doi: 10.1111/j.1582-4934.2009.00692.x PMID: 19220580

41. Piguet AC, Saar B, Hlushchuk R, St-Pierre MV, McSheehy PM, Radojevic V, et al. Everolimus augments the effects of sorafenib in a syngeneic orthotopic model of hepatocellular carcinoma. Molecular cancer therapeutics. 2011; 10(6):1007–17. doi: 10.1158/1535-7163.MCT-10-0666 PMID: 21487053

42. Wang WA, Groenendyk J, Michalak M. Endoplasmic reticulum stress associated responses in cancer. Biochimica et biophysica acta. 2014; 1843(10):2143–9. doi: 10.1016/j.bbamcr.2014.01.012 PMID: 24440276

43. Dai R, Chen R, Li H. Cross-talk between PI3K/Akt and MEK/ERK pathways mediates endoplasmic reticulum stress-induced cell cycle progression and cell death in human hepatocellular carcinoma cells. International journal of oncology. 2009; 34(6):1749–57. PMID: 19424594

44. Chow SE, Kao CH, Liu YT, Cheng ML, Yang YW, Huang YK, et al. Resveratrol induced ER expansion and ER caspase-mediated apoptosis in human nasopharyngeal carcinoma cells. Apoptosis: an international journal on programmed cell death. 2014; 19(3):527–41.

45. Zheng YZ, Cao ZG, Hu X, Shao ZM. The endoplasmic reticulum stress markers GRP78 and CHOP predict disease-free survival and responsiveness to chemotherapy in breast cancer. Breast cancer research and treatment. 2014; 145(2):349–58. doi: 10.1007/s10549-014-2967-x PMID: 24781973

46. Lei Y, Henderson BR, Emmanuel C, Harnett PR, deFazio A. Inhibition of ANKRD1 sensitizes human ovarian cancer cells to endoplasmic reticulum stress-induced apoptosis. Oncogene. 2015; 34(4):485–95. doi: 10.1038/onc.2013.566 PMID: 24531715

47. Chen J, Wei H, Xie B, Wang B, Cheng J. Endoplasmic reticulum stress contributes to arsenic trioxide-induced apoptosis in drug-sensitive and-resistant leukemia cells. Leukemia research. 2012; 36 (12):1526–35. doi: 10.1016/j.leukres.2012.08.018 PMID: 22959511

48. Brenner C, Galluzzi L, Kepp O, Kroemer G. Decoding cell death signals in liver inflammation. Journal of hepatology. 2013; 59(3):583–94. doi: 10.1016/j.jhep.2013.03.033 PMID: 23567086

49. Gao Y, Li HX, Xu LT, Wang P, Xu LY, Cohen L, et al. Bufalin enhances the anti-proliferative effect of sorafenib on human hepatocellular carcinoma cells through downregulation of ERK. Molecular biology reports. 2012; 39(2):1683–9. doi: 10.1007/s11033-011-0908-x PMID: 21617941

50. Rong X, Ni W, Liu Y, Wen J, Qian C, Sun L, et al. Bufalin, a bioactive component of the Chinese medicine chansu, inhibits inflammation and invasion of human rheumatoid arthritis fibroblast-like synoviocytes. Inflammation. 2014; 37(4):1050–8. doi: 10.1007/s10753-014-9828-y PMID: 24515724

51. Qi F, Inagaki Y, Gao B, Cui X, Xu H, Kokudo N, et al. Bufalin and cinobufagin induce apoptosis of human hepatocellular carcinoma cells via Fas- and mitochondria-mediated pathways. Cancer science. 2011; 102(5):951–8. doi: 10.1111/j.1349-7006.2011.01900.x PMID: 21288283

52. Zhang DM, Liu JS, Tang MK, Yiu A, Cao HH, Jiang L, et al. Bufotalin from Venenum Bufonis inhibits growth of multidrug resistant HepG2 cells through G2/M cell cycle arrest and apoptosis. European journal of pharmacology. 2012; 692(1–3):19–28. doi: 10.1016/j.ejphar.2012.06.045 PMID: 22841670

53. Chen YY, Lu HF, Hsu SC, Kuo CL, Chang SJ, Lin JJ, et al. Bufalin inhibits migration and invasion in human hepatocellular carcinoma SK-Hep1 cells through the inhibitions of NF-kB and matrix metalloproteinase-2/-9-signaling pathways. Environmental toxicology. 2015; 30(1):74–82. doi: 10.1002/tox.21896 PMID: 23949904

54. Hsu CM, Tsai Y, Wan L, Tsai FJ. Bufalin induces G2/M phase arrest and triggers autophagy via the TNF, JNK, BECN-1 and ATG8 pathway in human hepatoma cells. International journal of oncology. 2013; 43(1):338–48. doi: 10.3892/ijo.2013.1942 PMID: 23677253

55. Gu W, Liu L, Fang FF, Huang F, Cheng BB, Li B. Reversal effect of bufalin on multidrug resistance in human hepatocellular carcinoma BEL-7402/5-FU cells. Oncology reports. 2014; 31(1):216–22. doi: 10.3892/or.2013.2817 PMID: 24173654

56. Shen S, Zhang Y, Wang Z, Liu R, Gong X. Bufalin induces the interplay between apoptosis and autophagy in glioma cells through endoplasmic reticulum stress. International journal of biological sciences. 2014; 10(2):212–24. doi: 10.7150/ijbs.8056 PMID: 24550689